Pergamon

Geochimica et Cosmochimica Acta, Vol. 61, No. 8, pp. 1595–1611, 1997

0016-7037/97 $17.00 + .00

PII S0016-7037(97)00023-9

The albite-water system: Part IV. Diffusion modeling of leached and hydrogen-enriched layers

ROLAND HELLMANN

Crustal Fluids Group, L.G.I.T., C.N.R.S., Université J. Fourier, Observatoire de Grenoble, I.R.I.G.M. B.P. 53X, 38041 Grenoble Cedex, France

(*Received November* 3, 1995; *accepted in revised form January* 3, 1997)

Abstract—Measured H and Na concentration depth profiles in albite samples dissolved at 300°C at various pH conditions (Hellmann et al., 1997-Part III) are indicative of the complex nature of diffusion within leached/H-enriched layers. A qualitative comparison between the measured profiles and profiles based on various diffusion models reveals that the inward diffusion of H species and the outward diffusion of Na are not independent, but rather are interrelated by an interdiffusion process that can be modeled with a single interdiffusion coefficient $\tilde{D}$. The coefficient $\tilde{D}$ varies as a function of the concentration of either H or Na and is thus dependent on depth. The proposed interdiffusion model is based on rates of Na diffusion that are up to several orders of magnitude faster than H diffusion ($D_{Na}/D_H \gg 1$), this being in accord with direct diffusion measurements from the glass dissolution literature. Modeling results reveal that the rate of H diffusion is one of the most important parameters in determining the depths of leached/H-enriched layers. Based on a qualitative comparison between the measured profiles and the interdiffusion model, a lower limit of $D_H \geq 10^{-13}$ cm^2 s^{-1} can be estimated for leached/H-enriched layers created at acid pH (3.3–3.4) and 300°C. Depending on the estimated value of D_{Na}/D_H, this corresponds to $D_{Na} \gg 10^{-13}$ cm^2 s^{-1}. The use of a structural factor with $\tilde{D}$ imparts an even greater concentration dependence on the interdiffusion coefficient. Increasing the value of the structural factor has the effect of greatly increasing the depth of leaching/H enrichment for any given set of constant D_H and D_{Na}/D_H values. Irreversible chemical reactions which result in the uptake of H species, such as framework bond hydrolysis reactions, are also potentially important in correctly modeling diffusion of leached/H-enriched layers. Increasing the rate of reaction acts as a damping factor on steady-state diffusion profiles. Chemical reactions within leached/H-enriched layers potentially necessitate the addition of a chemical reaction term to the applied diffusion model in order to avoid an underestimation of diffusion rates. *Copyright © 1997 Elsevier Science Ltd*

1. INTRODUCTION

1.1. Diffusion in Leached/H-Enriched Layers

The present study is the fourth in a series devoted to the dissolution of albite at elevated temperatures and pressures. The preceding article in this issue entitled, "The albite-water system Part III. Characterization of leached and H-enriched layers formed at 300°C using MeV ion beam techniques," is a companion article; it is henceforth referred to simply as Part III. The main purpose of the present study is a better understanding of diffusion within leached and H-enriched zones that are formed during the dissolution of feldspars. Leached zones occur due to the preferential release of easily exchangeable interstitial cations from the bulk structure, such as Na, K, and Ca, as well as the preferential release of framework-forming elements, such as Al. Associated with this process of preferential leaching is the creation of H-enriched zones due to the large-scale permeation of the near-surface structure by H species from the aqueous solution. Since these processes occur concomitantly within the near-surface structure, they are often referred to together as a leached/H-enriched layer, or alternatively, simply as an altered layer. The formation of these altered layers is not solely restricted to feldspars; they also occur in certain other classes of minerals and glasses, as well. The depths of leached/H-enriched layers can range from a few tens of Å to many thousands of Å. In general, the specific conditions of dissolution, such as time, pH, temperature, solution composition, as well as the composition and structure of the mineral or glass, determine the depths of these altered layers (see Results and Discussion in Part III; and references therein).

The study of leached and H-enriched zones in minerals and glasses is important in understanding the overall dissolution process, both from a macroscopic point of view (i.e., measured laboratory rates), as well as the fundamental aspects of hydrolysis and detachment reactions at an atomic level. Leached/H-enriched zones in the near surface of minerals and glasses also play a potentially important role in the retention of trace and heavy elements (see Petit et al., 1990). This has important consequences with respect to the geochemical cycling and transport of these elements in natural environments (e.g., mid-ocean ridges). Aside from global geochemical cycles, leached and H-enriched layers that form during the dissolution of glasses (both natural and manmade) are important with respect to the retention of harmful radionuclides (Petit et al., 1990). Understanding the adsorption of such species in altered glass layers has an important bearing on modeling groundwater interactions with underground repository sites containing radwastes encapsulated in glasses.

Historically, there has been a debate as to the existence of leached/H-enriched layers. However, with the advent of

modern ion beam and spectroscopic/spectrometry techniques, their existence has been confirmed. Recent studies, using a variety of techniques, have documented in detail their chemical composition with depth (e.g., Berner and Holdren, 1979; Casey et al., 1988; Muir et al., 1989; Petit et al., 1990; Hellmann et al., 1990, Part III (see detailed discussion); Schweda and Sjöberg (1997); and references therein). The influence of these altered zones on dissolution kinetics has been debated for at least two decades. Altered layers, as well as secondary surface precipitates, that were observed to form as a response to weathering or hydrothermal alteration reactions were originally thought to play a role in retarding the overall dissolution process of minerals and glasses (see extensive discussion in Hellmann, 1995; Part III). Experimental evidence, however, showed that steady-state reactions were surface reaction controlled, and not diffusion-limited by transport of dissolved species through altered layers or precipitates. Nonetheless, current thinking is still rather divided on the importance of leached/H-enriched layers with respect to their influence on the overall rates of reaction of minerals and glasses (e.g., Brantley and Stillings, 1996; see also discussion of altered layers in Blum and Stillings, 1995).

One line of current thinking, which is the basis of this article, is that surface reactions control the overall rate of dissolution, but that these surface reactions are, in turn, influenced by reactions and processes occurring within leached and H-enriched zones, and vice versa (e.g., Hellmann, 1995; Part III). This hypothesis is termed surface reaction-leached layer kinetics (Hellmann, 1995). One of the keys to this interrelationship between the surface and the near surface is understanding how the inward and outward diffusion of elements operates within the near-surface altered zone, which extends from the surface to the unaltered bulk structure. Dynamic processes that occur during dissolution, such as the diffusion of species within a near-surface altered zone, have a potential influence on the chemical and physical properties of the surface. This leads to the premise that surface detachment reactions will occur at a rate that is influenced not only by the fluid/solid interface environment, but also by the structure and composition of leached and H-enriched layers that form between the surface and the bulk structure. Thus, knowledge of diffusional processes, which control the composition and structure of altered layers, is necessary for a complete understanding of the mechanisms and kinetic controls of dissolution reactions. Such information is crucial for correctly modeling dissolution reactions, particularly hydrolysis and detachment reactions on an atomic scale, such as with ab initio methods, etc.

When feldspars, similar minerals, and many glasses undergo dissolution reactions, the inward flux of H into the near-surface structure and the corresponding outward flux of interstitial and framework cations towards the fluid/solid interface can be characterized in terms of diffusion. The goal of the present study is to gain a better understanding of how H and interstitial cations diffuse within leached/H-enriched zones formed in feldspars. Specifically, various types of diffusion models are presented that are applicable to the outward diffusion of Na and the inward diffusion of aqueous H species. The diffusion profiles generated by these models are qualitatively compared to measured diffusion profiles in albite samples that were dissolved at acid pH conditions at 300°C (Results in Part III). This qualitative comparison allows for the following important aspects of diffusion in leached/H-enriched layers to be better understood: (1) the relative rates of diffusion, and which species is rate-limiting, (2) an estimation of diffusion rates, (3) the coupling between the inward and outward diffusion of species, (4) the influence of compositional/structural gradients on rates of diffusion, and (5) the influence of chemical reactions within the leached/H-enriched zone on rates of diffusion.

The Na and H diffusion profiles in altered albite samples were measured (Part III) by a MeV ion beam technique called Resonant Nuclear Reaction Analysis (RNRA). Information from this technique was complemented by qualitative results provided by two other MeV techniques, RBS and ERDA (also in Part III). The results and data from this study and Part III complement aqueous data obtained from two previous albite dissolution studies at elevated temperatures and pressures, the first pertaining to the pH-dependence of steady-state rates of dissolution (Hellmann, 1994; referred to as Part I), and the second pertaining to the stoichiometry of dissolution as a function of time (Hellmann, 1995; referred to as Part II).

It appears that the leaching of Na and the enrichment of H in albite dissolved at elevated temperatures at acid pH conditions extend to depths on the order of 1–2 μm (see Part III). However, the RNRA analyses did not extend beyond depths >6000 Å, and for this reason the full extent of Na leaching and H penetration is not known. This can be seen in Figs. 3 and 4a in Part III, which show incomplete H and Na profiles. These incomplete profiles did not warrant a direct comparison with the synthetic diffusion profiles derived in this study, which show the full extent of diffusion processes from the surface to the unaltered bulk structure. For this reason, no attempt has been made to actually model or fit equations to the measured profiles in order to obtain precise diffusion coefficients. Instead, the present study is based on the development of a series of diffusion models, starting with Fick's 2nd law. Successively more complicated diffusion models are presented, which include the use of nonconstant diffusion coefficients and the effects of chemical reaction. These models address many important questions regarding the interrelated behavior of Na and H diffusion. Most importantly, however, these diffusion models permit a qualitative comparison with the H and Na profiles and depths of alteration determined experimentally in Part III. This comparison is useful for gaining a better understanding of which parameters are important and which diffusion models are most accurate in describing the diffusion behavior of H and Na.

The comparisons are based on profiles obtained for dissolution at acid pH conditions (pH 3.4 and 300°C; diffusion profiles presented in Part III). The acid pH diffusion profiles were chosen since they show the greatest degree of Na depletion and H permeation. Nonetheless, the conclusions drawn from this comparison can just as well be applied to neutral pH conditions. However, for certain dissolution conditions, such as at basic pH, the thickness of the H-enriched region is insignificant (<1000 Å), such that caution is called for

when comparing experimental profiles with results from diffusion models.

As will be shown in the development of the diffusion models, the qualitative agreement between the models and the profiles is only approximate, but that is to be expected given the incomplete nature of the experimental profiles. This may also be due, in part, to diffusion models that are not yet sophisticated enough to incorporate all of the physical characteristics and chemical processes (i.e., diffusion and chemical reactions) that occur within leached/H-enriched layers formed at elevated temperatures. Thus, more work on this subject can be foreseen in the future. Nonetheless, it is important to note that the results from the present study already provide much important and new information on diffusion within feldspar leached/H-enriched zones. This information can also be applied to other minerals and glasses, where significant preferential leaching and/or H-enrichment occur during dissolution.

1.2. Previous Work

Even though leached/H-enriched layers in feldspars and other minerals have been confirmed by a variety of experimental methods, including both solution data and near-surface analytical techniques (see references in Introduction of Part III), little information is available in the literature concerning diffusion in leached/H-enriched layers in minerals and glasses. Chou and Wollast (1984) determined diffusion rates in altered layers formed on albite samples that were dissolved at 25°C at acid and neutral pH conditions. Using Fick's 1st law, they calculated Na diffusion rates that varied between 3.6×10^{-19} at acid pH (pH 1.2) and $10^{-20.0}$ $cm^2\ s^{-1}$ at neutral pH. A similar range exists for alkali diffusion rates in feldspars, extrapolated to 25°C, by Correns (1963), Wollast (1967), Pačes (1973), and Busenberg and Clemency (1976) (see values in Table 4 in Chou and Wollast, 1984). Significantly faster rates were found for Mg diffusion in Mg-silicates by Luce et al. (1972). As pointed out by Chou and Wollast (1984), however, a direct comparison of diffusion rates is difficult, owing to different mathematical assumptions, as well as the use of steady-state vs. nonsteady-state models.

In Part II, aqueous dissolution data were used to extrapolate diffusion rates of Na and Al at 100, 200, and 300°C. To briefly summarize the main findings, the extrapolated diffusion rates for Na and Al fit within an envelope of diffusion rates (see Fig. 11, Part II) bounded by Na diffusion in albite (i.e., the lower bound) and Na diffusion in albite glass (the upper bound). This was used as evidence that albite leached layers have transport properties intermediate between that of a crystalline and a glassy solid, which has a more open structure. It was also noted that the diffusion rates for Na and Al were of roughly the same magnitude. As was also shown in several past studies (e.g., Chou and Wollast, 1984; and references therein), the results in Part II show that the rates of diffusion in leached/H-enriched layers have a strong pH-dependence. The extrapolated rates of diffusion in layers created at very low acid pH conditions were as much as several orders of magnitude faster than those formed at neutral pH (see Fig. 12, Part II).

The problem inherent with the extrapolation of diffusion rates from aqueous data is that certain assumptions must be made concerning the shape of diffusion profiles. Often, a simple linear diffusion gradient is assumed (e.g., Chou and Wollast, 1984; Part II). As discussed in Parts II and III, this can lead to a significant underestimation of diffusion rates. Far more accurate determinations of diffusion rates are possible when diffusion models are applied to directly measured diffusion profiles. Sjöberg et al. (1995) measured H profiles by SIMS in plagioclases reacted at acid pH and 25°C. They also found a pH-dependency of the diffusion rates. Their H diffusion coefficients increase with decreasing pH from 10^{-18} to 10^{-16} $cm^2\ s^{-1}$ for reaction at pH 3 and 1, respectively. They also proposed an alternative diffusion model based on H diffusion and reaction within the leached/H-enriched zone. This led to a pH-invariant H diffusion coefficient of 10^{-12} $cm^2\ s^{-1}$. This value is many orders of magnitude faster than those reported in Table 4 of Chou and Wollast (1984). The results from Sjöberg et al. (1995) show that diffusion modeling of leached layers is not as straightforward as has been previously assumed.

2. DIFFUSION MODELING

2.1. Introduction

As is the case with most diffusion modeling, the point of departure is Fick's 2nd law, which for the case of one dimensional diffusion in a semi-infinite medium (for $x' > 0$) is expressed as

$$\frac{\partial C}{\partial t} = \frac{\partial}{\partial x'}\left(D\frac{\partial C}{\partial x'}\right) \quad (1)$$

where C is the concentration of the diffusing species, t is time, x' is the depth (positive distance from the fluid/solid interface into the solid), and D is the coefficient of diffusion. The solution to the above expression, using a Laplace transform method (see Crank, 1990), is relatively straightforward when the diffusion coefficient is constant. The solution, given below, is applied to the case of H diffusion into the near-surface structure, satisfying the boundary condition $C = C_0$ for $x' = 0$ and $t > 0$, and the initial condition $C = 0$ for $x' > 0$ and $t = 0$:

$$C = C_0 \operatorname{erfc} \frac{x'}{2\sqrt{(D_H t)}} \quad (2)$$

The general solution shown above gives the normalized concentration (i.e., C/C_0) of H as a function of time and depth for a given constant value of D_H. Figure 1 shows a set of diffusion profiles (based on Eqn. 2, with $D_H = 10^{-13}$ $cm^2\ s^{-1}$) representing H infiltration as a function of depth for various values of time.

The steady-state solution ($t = \infty$) is shown in Fig. 1 by the horizontal line representing a constant concentration of H as a function of depth. This type of a steady-state profile is not realistic for most samples, however, and is generally not very useful for describing diffusion profiles (H or Na) for steady-state dissolution conditions. The main reason for this is that diffusion is counterbalanced by other processes

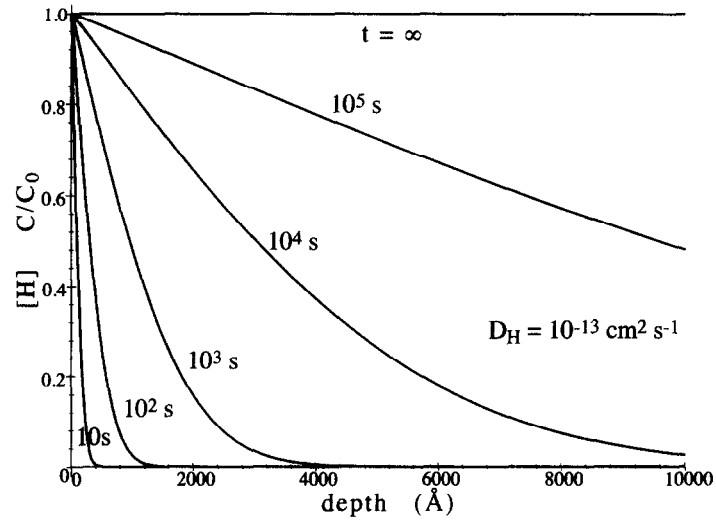

Fig. 1. The time evolution of H permeation of the near-surface structure, based on Eqn. 1 (see text) and $D_H = 10^{-13}$ cm^2 s^{-1}. Note that the values for [H] are normalized with respect to $[H]_0$ and that the fluid/solid interface is located at depth = 0; this holds true in this figure and all following figures. In this model the fluid/solid interface remains stationary. Short time solutions, such as shown, may be applicable to describing H diffusion profiles during the initial stages of dissolution, when the rate of diffusion ≫ rate of dissolution.

occurring during dissolution. One of these processes is the constant retreat of the fluid/solid interface during dissolution. Before discussing this further, however, it should be noted that short time solutions to the diffusion equation, given by Eqn. 2, may be applicable during the initial stages of dissolution, when the rate of diffusion is far greater than the rate of dissolution (see discussion in Lanford et al., 1979). In addition, Eqn. 2 may be used to describe diffusion when dissolution (i.e., the rate of retreat of the fluid/solid interface) is very slow, such as at neutral pH and 25°C.

2.2. Diffusion with a Moving Boundary

As mentioned above, the solution to the general diffusion equation, expressed by Eqn. 2, is only valid for a fixed coordinate system, and, therefore, does not account for the fluid/solid interface continuously retreating as a function of time during dissolution. Rewriting Eqn. 1 to account for a moving boundary necessitates a change in variables, based on the relation

$$x = x' - at \tag{3}$$

where x' is the distance of an arbitrary plane (within the altered structure) from the original fluid/solid interface (i.e., at $t = 0$), x is the distance of the same plane from the actual interface, and a is the rate of retreat of the interface. This change in coordinates ensures that $x = 0$ represents the fluid/solid interface at any time t. The general diffusion equation below accounts for a continuously moving boundary (Doremus, 1975)

$$\left(\frac{\partial C}{\partial t}\right) = \frac{\partial}{\partial x}\left(D\frac{\partial C}{\partial x}\right) + a\left(\frac{\partial C}{\partial x}\right) \tag{4}$$

where a is the rate of retreat of the fluid/solid interface.

In the following treatment of diffusion in leached/H-enriched layers, solutions to Eqn. 4 are presented, based on various diffusion models, ranging from simple to more complex cases. In all cases, the equations are solved for the steady-state condition. It is assumed that the measured concentration profiles of H and Na are invariant with time, and, therefore, the steady-state condition $\partial C/\partial t = 0$ is valid (see Discussion in Part III). In addition to the steady-state condition, the diffusion equations discussed below satisfy the following boundary conditions (note that concentrations are normalized to the bulk concentration): for H, at $x = 0$, $C_H = 1$ (the fluid/solid interface), and at $x = \infty$ (the H-enriched layer/bulk interface), $C_H = 0$ and $dC_H/dx = 0$; for Na, at $x = 0$, $C_{Na} = 0$, and at $x = \infty$ (the leached layer/bulk interface), $C_{Na} = 1$ and $dC_{Na}/dx = 0$. The boundary conditions $dC_H/dx = 0$ and $dC_{Na}/dx = 0$ at $x = \infty$ have been substantiated in numerous measured elemental depletion and H profiles (e.g., Casey et al., 1988; Petit et al., 1989b, Hellmann et al., 1990). Setting the boundary condition $C_{Na} = 0$ at the fluid/solid interface is based on experimental data. Many studies have shown that altered feldspars satisfy the condition $C_{Na} \approx 0$ (where Na is equivalent to K or Ca, depending on the feldspar) at the fluid/solid interface after dissolution in acid pH conditions, and occasionally also at neutral pH solutions (e.g., Petit et al., 1989b; Muir et al., 1990; Part III; Schweda and Sjöberg (1997)). In all cases, the rate of interface retreat a is set equal to 1 Å s^{-1} (based on the measured rate of dissolution at pH 3.4 and 300°C).

2.3. Constant *D*

The simplest case of diffusion with a moving boundary is based on constant values for D_H and D_{Na}. Taking Eqn. 4 and integrating twice with the appropriate boundary values, results in the following steady-state solutions for H and Na, respectively:

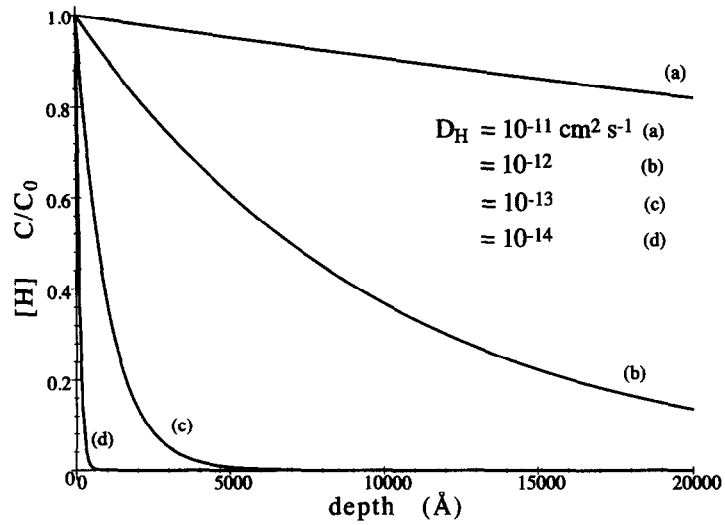

Fig. 2. Steady-state H diffusion profiles as a function of depth, based on values of D_H ranging from 10^{-11} to 10^{-14} $cm^2\ s^{-1}$. The exponentially decreasing profiles are based on Eqn. 5, where D_H is constant. Note that in this and all following figures, the diffusion profiles are based on a moving fluid/solid interface, with a rate of retreat equal to 1 Å s^{-1} (see text for details, Eqn. 4).

$$C_H = \exp\left(\frac{-ax}{D}\right) \quad (5)$$

$$C_{Na} = 1 - \exp\left(\frac{-ax}{D}\right) \quad (6)$$

Figures 2 and 3 show the calculated profiles for H and Na concentration vs. depth, respectively, based on the above equations. Each figure shows several diffusion profiles, corresponding to constant diffusion coefficients, D_H and D_{Na}, that range from 10^{-11} to 10^{-14} $cm^2\ s^{-1}$. This range for D_{Na} agrees well with the experimentally determined range of values at 300°C reported in Part II ($D_{Na} \approx 10^{-12}$ to 10^{-15} $cm^2\ s^{-1}$; see Fig. 11, Part II). The calculated profiles shown in Figs. 2 and 3 show H infiltration and Na depletion occurring to depths of several thousand Å when the respective diffusion coefficients are greater than 10^{-14} $cm^2\ s^{-1}$. Values of $D_{Na,H} < 10^{-14}$ $cm^2\ s^{-1}$ yield Na and H profiles that are representative of leached/H-enriched layers that are at most only several hundred Å thick.

The curves in Figs. 2 and 3 display characteristic exponential behavior often encountered in the literature for tracer and self-diffusion experiments. Boksay et al. (1967, 1968) used Eqn. 6 to model the distribution of cations in leached layers occurring in glasses. However, the exponential form of the calculated curves does not resemble the sigmoidal profiles that have been measured by a variety of techniques in altered feldspars (see references in next section). In a

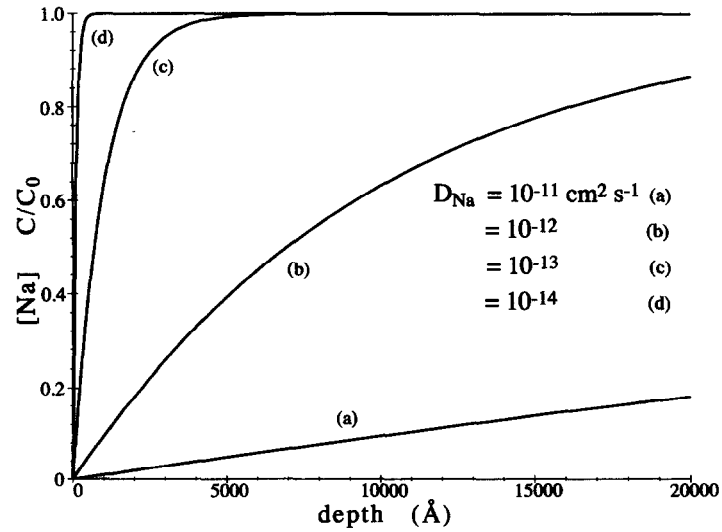

Fig. 3. Steady-state Na diffusion profiles as a function of depth, based on values of D_{Na} ranging from 10^{-11} to 10^{-14} $cm^2\ s^{-1}$. The exponentially increasing profiles are based on Eqn. 6, where D_{Na} is constant.

study of a naturally hydrated obsidian by Lee et al. (1974), the RNRA data also show a very distinct sigmoidal H profile. Doremus (1975), in modeling the outward diffusion of alkalis in alkali silicate glasses, also noted that exponential profiles do not produce a satisfactory fit of experimentally-measured diffusion profiles. This mismatch was attributed to modeling the diffusion process with a constant diffusion coefficient in Eqn. 4.

2.4. Interdiffusion Coefficient $\tilde{D}$

As discussed above, the use of constant diffusion coefficients for H and Na does not reproduce the general behavior of experimentally determined diffusion curves in altered feldspars, as well as in other silicates and glasses. With respect to albite, this is due to the fact that the outward diffusion of Na and the inward diffusion of H are not independent, but rather are coupled by an ion exchange reaction between H^+ (or H_3O^+) and Na^+ (see Part II, and references therein). Experimental evidence for the interdependent nature of Na and H diffusion can be found in Petit et al. (1989b). In their study they noted a suppression of Na loss as well as a marked decrease in H penetration when feldspars were dissolved in solutions spiked with elevated concentrations of Na. The anticorrelative nature of the H and Na RNRA profiles in Part III (Figs. 3 and 4a) also suggest ion exchange between H and Na.

To take into account this interdependency necessitates the use of a nonconstant diffusion coefficient in the diffusion equation given in Eqn. 4. For the case of binary (2 components) diffusion, it was shown by Darken (1948) and Hartley and Crank (1949) that the diffusion behavior of such a system can be described by a single interdiffusion coefficient (also called a mutual diffusion coefficient), where the interdiffusion coefficient varies as a function of the concentration of the diffusing species. The following expression can be used to describe binary cation diffusion behavior in silicate minerals (from Brady, 1995; see original references therein):

$$D_{A_bB_{-a}} = \left[\frac{(D^*_{AZ})(D^*_{BZ})(aN_{AZ} + bN_{BZ})^2}{(a^2N_{AZ}D^*_{AZ} + b^2N_{BZ}D^*_{BZ})}\right] \times \left[1 + \left(\frac{\partial \ln \gamma_{AZ}}{\partial \ln N_{AZ}}\right)_{P,T}\right] \quad (7a)$$

where the reaction is $A_z^{+a}Z_a^{-z} \leftrightarrow B_z^{+b}Z_b^{-z}$, D^*_{AZ} and D^*_{BZ} are the respective tracer diffusion coefficients for phases AZ and BZ, and N_{AZ} and N_{BZ} are the mole fractions for each phase (for a generalized relationship concerning diffusion in multicomponent minerals, see Lasaga, 1979). For the case of $^+a = {}^+b$, and neglecting the activity coefficient term ($\gamma_{AZ} \approx 1$), then the interdiffusion coefficient given by Eqn. 7a can be expressed in terms of H and Na interdiffusion as follows (Baucke, 1974; Doremus, 1975):

$$\tilde{D} = \frac{D_{Na}D_H}{C_{Na}D_{Na} + (1 - C_{Na})D_H} = \frac{D_{Na}}{1 + C_{Na}b} \quad (7b)$$

where D_{Na} and D_H are individual diffusion coefficients, C_{Na} is the bulk normalized concentration of Na, and $b = (D_{Na}/D_H) - 1$. The interdiffusion model presented here assumes that the diffusive fluxes of H and Na are equal and opposite. It is important to note that in this model, the diffusion coefficients D_{Na} and D_H are invariant with concentration and depth.

Note that in the expression above, $\tilde{D}$ varies in a nonlinear fashion with concentration, and by implication, with depth as well. The variation of $\tilde{D}$ as a function of C_{Na} is shown in Fig. 4 (curve corresponding to $\alpha = 0$). Note that the sharp decrease in the log normalized value of $\tilde{D}$ over the range $C_{Na} = 0$–0.2 implies that the rates of H and Na interdiffusion are significantly faster, by more than 2 orders of magnitude, close to the fluid/solid interface as compared to deeper within the leached layer structure.

Substituting $\tilde{D}$ for D in Eqn. 4 and integrating twice, subject to the appropriate boundary conditions, results in the following solution relating C_{Na} to depth (Doremus, 1975):

$$C_{Na} = \frac{[1 - \exp(-ax/D_H)]}{[1 + b\exp(-ax/D_H)]} \quad (8)$$

where $b = (D_{Na}/D_H) - 1$ (note that Eqn. 8 corrects for a sign error in the numerator of Eqn. 9, Doremus, 1975).

Figure 6a shows a series of Na interdiffusion profiles based on Eqn. 8. The corresponding H interdiffusion profiles are shown in Fig. 5. Note that the H profiles were also calculated from Eqn. 8, using the relation $C_H = 1 - C_{Na}$. The most important difference between these profiles and the preceding ones (Figs. 2, 3) is their sigmoidal behavior. Note that all of the profiles are sigmoidal (curves d–h in Figs. 5, 6a), except for the profiles based on $D_{Na}/D_H \leq 1$ (curves a–c), which show exponential behavior. When $D_{Na}/D_H = 1$, such that $b = 0$ in Eqn. 8, Eqn. 8 reduces to Eqn. 6 (which also requires an exchange of the H and Na diffusion coefficients). The important point to note is that sigmoidal diffusion profiles, when based on diffusion defined by Eqn. 4 and an interdiffusion coefficient corresponding to Eqn. 7b, require $D_{Na}/D_H > 1$.

The sigmoidal H and Na diffusion profiles in Figs. 5 and 6a are in much better accord with measured leaching and H enrichment profiles of altered feldspars found in the literature; the same holds for many silicates and silicate glasses, as well (see examples in Baucke, 1974; Lanford et al., 1979; Smets and Lommen, 1982; Dran et al., 1988; Petit et al., 1989a,b, 1990; Hellmann et al., 1990; Schweda and Sjöberg, 1997). Apparent exceptions to this are discussed further on in the Discussion and Summary section.

The sigmoidal diffusion profiles in Figs. 5 and 6a are based on D_{Na}/D_H ratios ranging from 10^1 to 10^5. These values imply a greater diffusivity of alkalis with respect to hydrogen species. Although the relative H and Na diffusivities were not measured in the present study, data from silicate glass dissolution studies show a far greater diffusive mobility of alkalis vs. hydrogen species, by several orders of magnitude (see Baucke, 1974; Lanford et al., 1979; Smets and Lommen, 1982; and references therein). The greater mobility of Na vs. H can be ascribed to the greater number of adsorption sites available to diffusing H species, such as bridging oxygen sites and metal-OH groups within the leached/H-enriched layers. Adsorption serves to decrease the effective rate of diffusion.

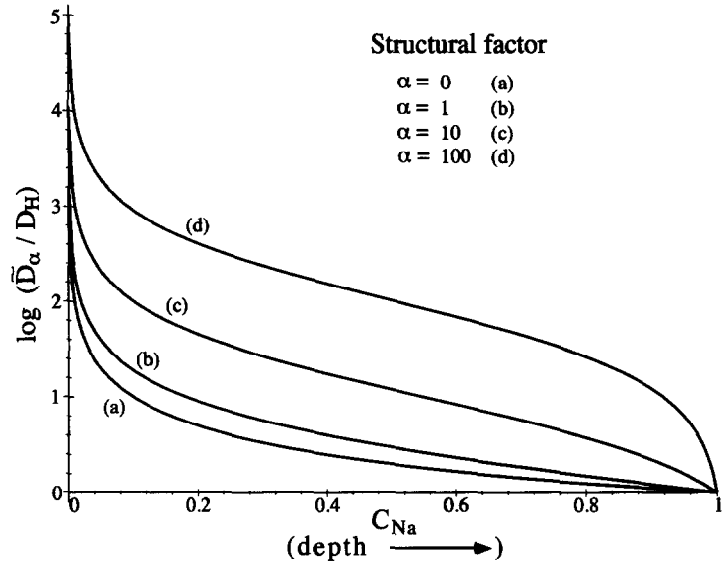

Fig. 4. The variation of the log normalized interdiffusion coefficient as a function of normalized Na concentration, and by implication, depth (increasing, left to right). Note that with increasing values of the structural factor (α), the nonlinearity of the diffusion rate as a function of [Na] and depth increases (see Eqn. 9 and text for details).

The H and Na diffusion profiles shown in Figs. 5 and 6a can be used to estimate rates of H and Na diffusion in the altered zone, based on data for Na leaching and H penetration depths presented in Part III. Note that three depth scales are given in each of the figures. The maximum depths and the specified D_H values ($cm^2\ s^{-1}$) for each depth scale are as follows: 2,000 Å ($D_H = 10^{-14}$); 20,000 Å ($D_H = 10^{-13}$) and 200,000 Å ($D_H = 10^{-12}$). Values for D_{Na} are a function of the ratio D_{Na}/D_H. Based on the H RNRA data given in Part III (see Fig. 3), the H plateau extends to depths >6000 Å. The ERDA data presented in Part III (see Fig. 9), while not quantitative with respect to absolute H concentrations, do show a continuous amount of H enrichment over a depth of at least ~1 μm (10,000 Å). Similarly, even though the Na RBS data in Part III are also not quantitative, Na depletion also extends to significant depths, on the order of 2μm

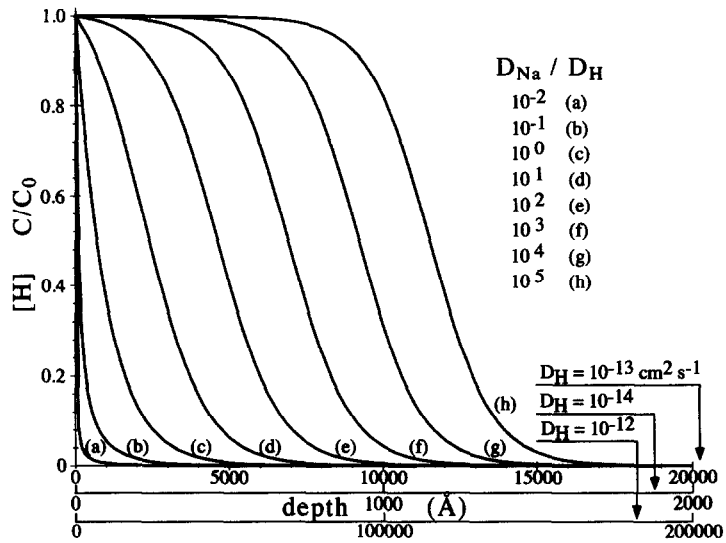

Fig. 5. Steady-state H diffusion profiles based on H and Na interdiffusion (see Eqn. 8 and text). The profiles are plotted as a function of depth and various values of D_{Na}/D_H. The interdiffusion coefficient is not a constant but varies as a function of depth and concentration (see $\alpha = 0$ curve in Fig. 4). Note the depths of H penetration are a strong function of D_H, while a much weaker function of D_{Na}/D_H. The maximum depths along the x axis are evaluated in terms of three different values of D_H, resulting in maximum depth scales ranging from 2,000 to 200,000 Å. Note that the diffusion profiles display either exponential behavior, when $D_{Na}/D_H \leq 1$, or sigmoidal behavior when $D_{Na}/D_H > 1$. Based on a comparison with the acid pH results in Part III, a lower bound of $D_H \geq 10^{-13}\ cm^2\ s^{-1}$ can be estimated.

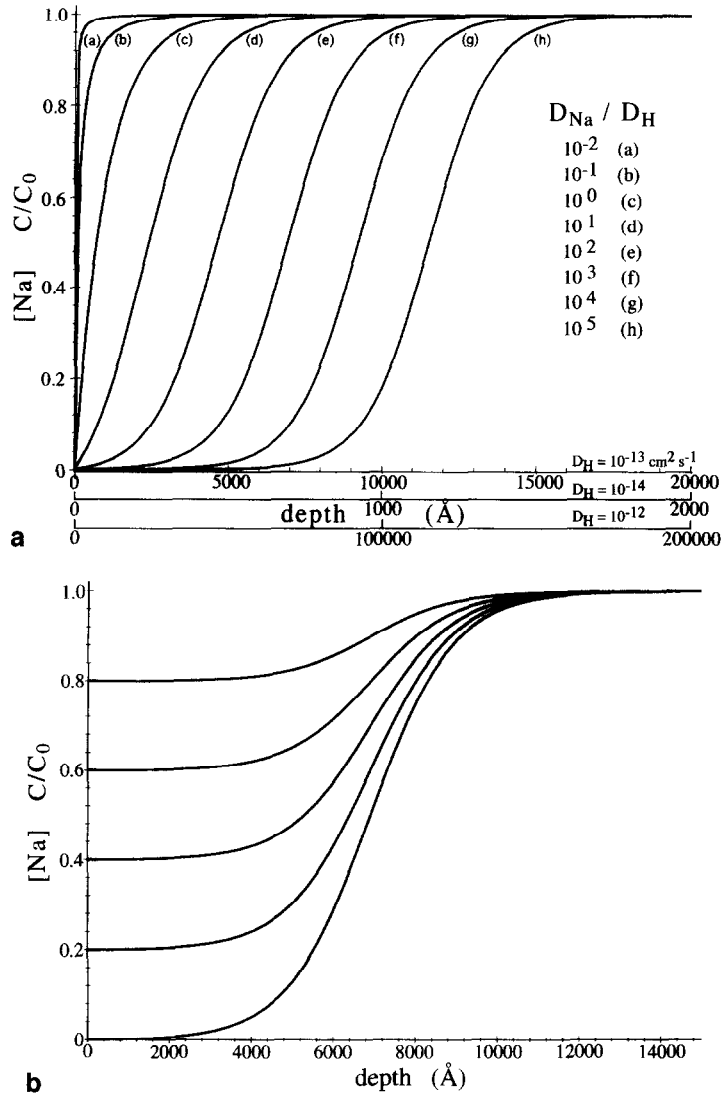

Fig. 6. (a) Steady-state Na diffusion profiles based on H and Na interdiffusion (see Eqn. 8). Note the increasing depth of Na depletion with increasing D_H and increasing D_{Na}/D_H. See Fig. 5 caption for more details concerning the interpretation of the diffusion profiles. (b) The effect of increasing the value of $C_{Na\ min}$ at the fluid/solid interface is shown by this family of steady-state Na interdiffusion profiles ($D_H = 10^{-13}$ cm^2 s^{-1}, and $D_{Na}/D_H = 1000$ for all profiles). Note that the slope of the sigmoidal diffusion front becomes shallower and that the overall amount of Na lost by diffusion decreases with increasing values of $C_{Na\ min}$.

(see discussion on limitations of data in Part III). Based on these estimates for H enrichment and Na depletion depths, the most reasonable choice for D_H is $\geq 10^{-13}$ cm^2 s^{-1}. As can be seen in Figs. 5 and 6a, it is more difficult to estimate the value of D_{Na}, given the lack of exact depths of Na leaching and H enrichment in Part III. Nonetheless, it seems reasonable to estimate that $D_{Na}/D_H \gg 1$. This estimate, according to Figs. 5 and 6a, yields reasonable depth estimates for both H enrichment and Na depletion that are compatible with the data in Part III.

It is interesting to note that the overall depths of H enrichment are not as sensitive to the ratio D_{Na}/D_H as they are to the value of D_H. This can be easily demonstrated by examining Fig. 5 and choosing two different values of D_{Na}/D_H, with $D_H = 10^{-13}$ cm^2 s^{-1} remaining fixed. For example, when $D_{Na}/D_H = 10^2$ (curve e), H penetration extends to ~10,000 Å; this can be compared to $D_{Na}/D_H = 10^4$ (curve g), in which case H penetration extends to ~15,000 Å. This shows that an increase of 10^2 in D_{Na} increases the depth of H penetration by only ~5,000 Å. The same type of result holds for Na depths of depletion. On the other hand, a change of D_H by an order of magnitude also changes the corresponding Na and H depths by an order of magnitude (for a constant ratio D_{Na}/D_H). The implication for this is quite important in that it demonstrates that the value of D_H plays a dominant role in determining Na leaching and H penetration depths, based on an interdiffusion coefficient of the form given by Eqn. 7b.

In the discussion earlier concerning boundary conditions and parameters as applied to the general form of the diffusion

equation (Eqn. 4), it was stated that $C_{Na\,min} = 0$ at the fluid/solid interface (i.e., depth $x = 0$) is generally applicable, as based on experimental evidence on feldspar (albite) dissolution at acid pH conditions. As shown in Part III (see Fig. 4a), however, this doesn't necessarily hold true at other pH conditions of dissolution, such as at neutral pH. For the case where $C_{Na\,min} > 0$, the Na interdiffusion profiles still retain their sigmoidal shape, however. What does change is the nature of the diffusion front. Figure 6b illustrates this with a family of Na interdiffusion profiles, corresponding to $C_{Na\,min}$ ranging from 0 to 0.8 at $x = 0$ (all diffusion profiles are based on $D_H = 10^{-13}$ cm^2 s^{-1}, and $D_{Na}/D_H = 1000$). A comparison of the profiles reveals that increasing the value of $C_{Na\,min}$ results in the diffusion front becoming shallower. The overall depths of Na depletion in all cases remain the same, but the overall amount of Na depletion necessarily decreases with increasing values of $C_{Na\,min}$. The calculation of diffusion profiles, where $C_{Na\,min} > 0$, is based on a simple mathematical transformation given by $C'(x) = C_{Na\,min} + (1 - C_{Na\,min})C(x)$, where $C'(x)$ is the concentration of Na at depth x for a given value of $C_{Na\,min}$, and $C(x)$ is the concentration of Na at depth x corresponding to $C_{Na\,min} = 0$.

2.5. Interdiffusion Coefficient $\tilde{D}_\alpha$, Incorporation of a Structural Factor (α)

Despite the fact that the calculated profiles shown in Figs. 5 and 6a display sigmoidal behavior and depths of alteration that are physically reasonable, one question that should be addressed concerns itself with the (speculative) situation of H-enrichment and Na depletion being significantly greater than ~17,000 Å. Based on Figs. 5 and 6a, ~17,000 Å of Na leaching and H enrichment corresponds to the maximum attainable alteration depth, with $D_H = 10^{-13}$ cm^2 s^{-1} and $D_{Na}/D_H = 10^5$. An increase in alteration depths can be effected in a variety of ways. One way of extending alteration depths is simply to further increase either the ratio D_{Na}/D_H, or the rate of diffusion of H, such that $D_H = 10^{-12}$ cm^2 s^{-1}, for example. Note that changing the latter has by far the greatest effect on increasing the depth of alteration. Another means of achieving this is by the introduction of a structural factor, denoted by α. The introduction of such a factor provides a mathematical means of increasing the mobility of diffusing species close to the fluid/solid interface, without increasing the values of the individual diffusion coefficients, D_{Na} and D_H.

The use of α is not purely mathematical, however. The physical significance of α is to increase the concentration (i.e., depth) dependence of the interdiffusion coefficient. As will be shown below, the use of this structural factor allows the rate of Na and H interdiffusion to dramatically increase towards the fluid/solid interface. This is based on the premise that as the leached/H-enriched zone progresses into the structure, the leached/H-enriched region close to the fluid/solid interface becomes more open, thereby allowing faster rates of interdiffusion.

As an example of this, Lanford et al. (1979) modeled diffusion curves in altered glasses that were measured as a function of time. Using the diffusion model described below, they obtained best fits to their diffusion data by increasing α from 1 to 10 for profiles that were obtained as a function of time. They noted that this could be attributed to structural changes and stresses which built up with increasing time in the leached/H-enriched zone during the dissolution of the glass. In the present study, the use of an interdiffusion coefficient with a structural factor provides a steady-state diffusion model which allows for significantly higher degrees of H penetration and Na loss simply by dramatically increasing the mobility of these species close to the fluid/solid interface.

A structural-interdiffusion coefficient can be formulated by letting $\tilde{D}$ vary linearly as a function of concentration (C_H in this case) and α, as shown in the following equation (from Lanford et al., 1979):

$$\tilde{D}_\alpha = (1 + \alpha C_H)\tilde{D} = \frac{(1 + \alpha C_H)}{(1 + bC_H)} D_H \qquad (9)$$

In Eqn. 9, α is an adjustable parameter and $b = (D_H/D_{Na}) - 1$. As compared to $\tilde{D}$ in Eqn. 7b, the additional concentration dependence of $\tilde{D}_\alpha$ is a function of multiplication of $\tilde{D}$ by the term $(1 + \alpha C_H)$.

Figure 4 shows the effective diffusion coefficient ($\log \tilde{D}_\alpha/D_H$) as a function of C_{Na} and the parameter α (for $D_H/D_{Na} = 0.001$). Note that in Fig. 4, C_{Na} rather than C_H was used, thereby allowing the depth into the leached/H-enriched layer to increase from left to right (i.e., $C_{Na} = 0$ corresponds to the fluid/solid interface). The curves in Fig. 4 show that as α increases, the rate of interdiffusion increases for any given value of C_{Na}. When $\alpha = 10$, the effective interdiffusion coefficient decreases by ~4 orders of magnitude between the fluid/solid interface and the bulk structure. Note that the influence of α on the rate of diffusion decreases with increasing depth into the structure, such that all of the curves converge at $C_{Na} = 1$, which represents the interface between the leached/H-enriched altered layer and the unaltered bulk structure.

The diffusion profiles for H and Na can be determined by substituting $\tilde{D}_\alpha$ from Eqn. 9 into Eqn. 4, integrating twice and applying the appropriate boundary conditions. The resulting expression (adapted from Lanford et al., 1979)

$$(-ax/D_H) = \ln [C_H] + \frac{(\alpha - b)}{b} \ln [(1 + bC_H)/(1 + b)] \qquad (10)$$

can be used to determine the relationship between C_H and the depth x (and C_{Na}, since $C_{Na} = 1 - C_H$). The effect of the parameter α on the diffusion profiles, for both H and Na, is shown in Figs. 7 and 8, respectively. The diffusion profiles are based on $D_H = 10^{-13}$ cm^2 s^{-1} and $D_{Na}/D_H = 10^3$. When $\alpha = 0$, the diffusion profiles represent simple interdiffusion, where the effective interdiffusion coefficient does not depend on a structural factor (as illustrated in Figs. 5 and 6). Increasing the value of α significantly increases both the depths of H penetration (Fig. 7) and Na leaching (Fig. 8). For example, in Fig. 7, an increase in α from 0 to 3 changes the depth of H penetration from ~15,000 Å to ~35,000 Å, a more than twofold increase. By analogy, the same increase in α produces an equivalent increase in the Na leaching depth (see Fig. 8).

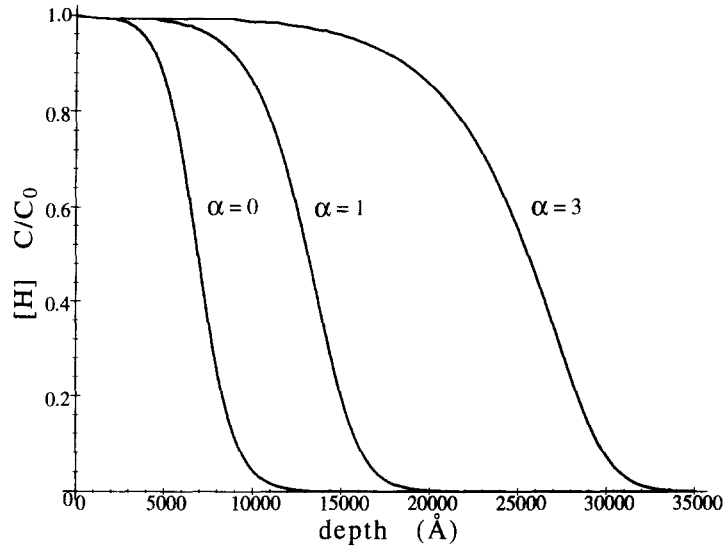

Fig. 7. Steady-state H diffusion profiles based on H and Na interdiffusion, where the interdiffusion coefficient is modified by a structural factor α (see Eqn. 9). This structural factor serves to account for changing transport characteristics of the leached/H-enriched layers as a function of depth (see Fig. 4). Note the increasing extent of the H penetration as a function of the value of α. The diffusion profiles are based on $D_H = 10^{-13}$ cm^2 s^{-1} and $D_{Na}/D_H = 1000$.

The most important point to note in Figs. 7 and 8 is that with increasing α, the depths of H infiltration and Na loss can be significantly increased, without changing the individual diffusion coefficients for H and Na. This follows as a direct consequence of the linear dependence of the depth x on α, as can be seen in Eqn. 10. The use of an interdiffusion coefficient with a structural factor in the diffusion equation is reasonable if one assumes that diffusion coefficients have a strong dependence on concentration and distance within the leached/H-enriched zone, especially close to the surface.

2.6. Diffusion and Chemical Reaction

One of the simplifying assumptions made in applying the preceding interdiffusion models is that the fluxes of H and Na are equal and opposite within the leached/H-enriched structure. However, the interdiffusion of H and Na species is not the sole process associated with H penetration. As was noted in Part III, the experimental data at acid pH show that the amount of H incorporated in the structure far exceeds the amount of Na lost (see Fig. 10, Part III). This imbalance

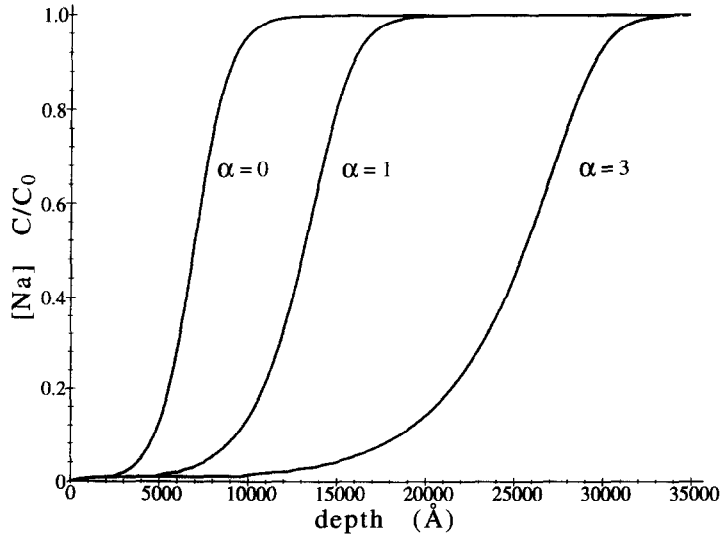

Fig. 8. Steady-state Na diffusion profiles based on H and Na interdiffusion, where the interdiffusion coefficient is modified by a structural factor α (see Eqn. 9). Note the increasing depth of Na depletion with increasing values of α. For more details, see Fig. 7 caption.

is due mainly to the uptake of H associated with framework hydrolysis reactions during dissolution (see Part III for details).

Until now, the situation of simultaneous diffusion and chemical reaction occurring within the leached/H-enriched zone has not been addressed. In general, chemical reactions will affect the diffusion of H species to a far greater degree than Na due to the preponderance of reaction sites susceptible to interactions with H species. Adsorption and reaction of H species in feldspars should primarily occur at bridging oxygen (O_{br}) sites in ≡Al—O—Si≡ and ≡Si—O—Si≡ linkages (Xiao and Lasaga, 1994; and references therein), as well as at ≡Si—OH and ≡Al—OH groups that are created by hydrolysis reactions (note that protonation and deprotonation reactions of these metal-OH groups is pH and temperature dependent; see discussion in Part III).

In general, the uptake of H species by chemical reaction decreases the concentration of species free to diffuse, thereby necessitating an additional term in the general diffusion equation given by Eqn. 4. In the discussion below, we examine how the immobilization of H species by chemical reaction affects the steady-state diffusion profiles of H and Na. Two general types of chemical reactions will be analyzed: reversible and irreversible reactions.

2.6.1. *Reversible chemical reactions*

Taking the case where the rate of reaction of a diffusing species is reversible and very much greater than the rate of diffusion, then one can assume the existence of a local equilibrium between free and reacted species. This situation, for example, occurs when H species are adsorbed at ≡Al—OH and ≡Si—OH sites within the leached/H-enriched region. The simplest case can be described by a linear adsorption isotherm (using the notation of Crank, 1990, and applying it to H adsorption)

$$S = RC \tag{11}$$

where S is the concentration of H immobilized by reaction, R is the equilibrium constant for the reaction, and C is the concentration of H free to diffuse.

The effect of the time-dependent uptake (reaction) of H at adsorption sites necessitates the subtraction of the additional term, $\partial S/\partial t$, from $\partial C/\partial t$ in Eqn. 4. The general diffusion equation becomes

$$\left(\frac{\partial C}{\partial t}\right) = \frac{\partial}{\partial x}\left(D\frac{\partial C}{\partial x}\right) + a\left(\frac{\partial C}{\partial x}\right) - \frac{\partial S}{\partial t} \tag{12}$$

Substituting Eqn. 11 into Eqn. 12, and writing the expression with respect to H infiltration results in

$$\left(\frac{\partial C_H}{\partial t}\right) = \left(\frac{1}{1+R}\right)\frac{\partial}{\partial x}\left(D\frac{\partial C_H}{\partial x}\right) + \frac{a}{1+R}\left(\frac{\partial C_H}{\partial x}\right) \tag{13}$$

As can be immediately deduced from the above equation, the effect of H adsorption and reaction is to reduce the effective diffusion coefficient D by a factor of $1/(1 + R)$, thereby reducing the rate of diffusion.

The time-dependent solution to Eqn. 13 can be solved using the same methods as for diffusion without chemical reaction. However, in our case, the time-independent solution is of interest. Under steady-state conditions, $\partial C_H/\partial t = 0$, and, therefore, the $1/(1 + R)$ terms drop out, resulting in the following differential equation:

$$\frac{\partial}{\partial x}\left(D\frac{\partial C_H}{\partial x}\right) + a\frac{\partial C_H}{\partial x} = 0 \tag{14}$$

The analytical solution to the above equation has been given earlier for various choices of D.

The interesting result is that the steady-state solution is not affected by the reaction of H at adsorption sites, provided that the reaction is instantaneous and that the linear adsorption isotherm given by Eqn. 11 holds. Thus, the steady-state profile for H diffusion, with or without a constant diffusion coefficient, will be the same for a given set of boundary conditions, regardless of whether or not H is consumed by an instantaneous chemical reaction, as given by Eqn. 11.

In a similar manner, the effect of a nonlinear adsorption process can be investigated. A nonlinear isotherm can be represented by

$$S = RC^n \tag{15}$$

The general diffusion equation, with Eqn. 15 substituted into Eqn. 12, can be represented as follows:

$$\frac{\partial C}{\partial t} = \frac{\partial}{\partial x}\left(D\frac{\partial C}{\partial x}\right) + a\frac{\partial C}{\partial x} - Rn(C)^{n-1}\frac{\partial C}{\partial t} \tag{16}$$

Time-dependent solutions of the above equation require numerical methods of integration (see Crank, 1990; and references therein). However, at steady-state, $\partial C_H/\partial t = 0$, and, therefore, Eqn. 16 reduces to Eqn. 14. As was the case with linear adsorption, there is no effect of nonlinear H adsorption on the steady-state H diffusion profile.

Thus, one can generalize from the two examples given: adsorption of H will slow down the diffusion rate but will not have any effect on steady-state diffusion profiles. The two conditions necessary for this result to hold is that adsorption is a reversible process and that the rate is more rapid than diffusion. These two conditions result in a localized equilibrium between diffusing species and species immobilized by reaction (Crank, 1990). The important point is that under such conditions, the overall process of infiltration (H species or any other species) is diffusion controlled, and steady-state diffusion profiles are unaffected by chemical reactions.

2.6.2. *Irreversible chemical reactions*

The two cases discussed above, where the rate of chemical reaction is reversible and much faster than diffusion, is probably not applicable to H adsorption and reaction at bridging O sites. This type of a process can represented by the following irreversible chemical reaction (at acid pH): ≡Si—O—Al≡ + H_3O^+ → ≡Al—OH_2^+ + ≡Si—OH. This overall, generalized reaction represents the fundamental process associated with framework bond hydrolysis, Al preferential release, and the concomitant creation of Al leached layers. In this case, there is no macroscopic chemical equilibrium between free H species and H species immobilized by

reaction at bridging O sites, resulting in bond hydrolysis and the formation of reaction products, such as ≡Al—OH_2^+ and ≡Si—OH. If the rate of uptake of H, given by $(\partial S/\partial t)$, is represented by a first order rate equation, then the following relation holds:

$$r = kC = \partial S/\partial t \qquad (17)$$

where r is the rate of reaction, k is the rate constant, and C is the concentration of diffusing H species. Substitution of Eqn. 17 into the diffusion equation given by Eqn. 12 results in the following expression for irreversible H uptake at steadystate:

$$0 = \left(\frac{\partial C_H}{\partial t}\right) = \left(\frac{\partial}{\partial x}\right)\left(D\frac{\partial C_H}{\partial x}\right) + a\left(\frac{\partial C_H}{\partial x}\right) - kC_H \qquad (18)$$

The solution to Eqn. 18 is not trivial when the H diffusion coefficient D is not a constant. On the other hand, when D is considered to be constant, integration of Eqn. 18, with the same boundary conditions applied previously to H diffusion, results in the following steady-state solution (Maple® software):

$$\frac{C}{C_0} = \exp\left\{\frac{(a + \sqrt{a^2 + 4Dk})x}{-2D}\right\} \qquad (19)$$

Figure 9 shows the effect of H uptake by irreversible chemical reaction on H diffusion profiles. As mentioned earlier, the primary reaction mechanism for this is the irreversible hydrolysis of framework elements, mainly associated with ≡Al—O—Si≡ groups and the subsequent release of Al (aqueous?) within the leached/H-enriched zone. Since Na does not participate in reactions of this type, no Na profiles are shown. The H profiles shown are based on the rate of retreat a of the fluid/solid interface equal to 1 Å s^{-1}. The profiles consist of a family of diffusion curves, corresponding to constant D_H values of 10^{-11} and 10^{-12} cm^2 s^{-1}, respectively. For a given value of D_H, several curves are shown, corresponding to values of the rate constant k ranging from 0 to 10^{-3} s^{-1}. As k increases in value, the values of C/C_0 decrease correspondingly for a given specified depth. Thus, the net effect of k (i.e., irreversible chemical reaction) is to act as a damping factor for the steady-state diffusion process.

The results shown in Fig. 9 have several important implications with respect to the influence of k on the depth of H penetration. First, with increasing k, the depth of H penetration is decreased. An example of this can be seen in the curves representing $D_H = 10^{-12}$ cm^2 s^{-1}. Note that for $k = 10^{-3}$ s^{-1}, the depth of H penetration is ~15,000 Å. For values of $k < 10^{-4}$ s^{-1}, the depths of H penetration extend to depths >30,000 Å (note that in Fig. 9 the profiles are not shown beyond $x > 30{,}000$ Å). The second important point is that the damping effect of k depends on the value of D_H. A comparison of the diffusion profiles at a depth of 15,000 Å reveals that the difference in C/C_0 between $k = 0$ and $k = 10^{-4}$ s^{-1} is far more pronounced for $D_H = 10^{-11}$ than is the case for $D_H = 10^{-12}$ cm^2 s^{-1}. Therefore, the higher the rate of H diffusion, the greater is the damping effect due to chemical reaction within the altered zone.

The corresponding H diffusion curves that result from the incorporation of a nonconstant diffusion coefficient (e.g., an interdiffusion coefficient $\tilde{D}$) into Eqn. 18 have not been calculated. However, the damping effect of the k term should be analogous to that shown for the case of a constant D_H in Fig. 9. One can make the generalization that diffusion combined with irreversible chemical reactions can significantly change steady-state diffusion profiles. This point is amply demonstrated with the H profiles shown in Fig. 9. This underlines the importance of including a kinetic term in diffusion models when a diffusing species is subject to

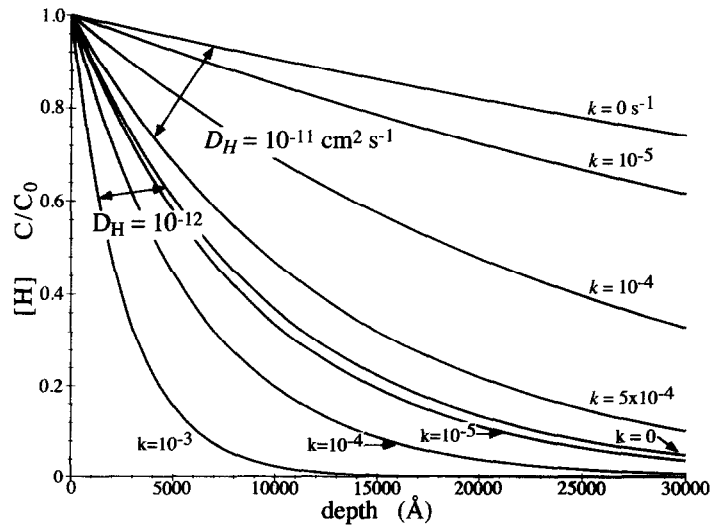

Fig. 9. Steady-state H diffusion profiles showing the effect of H uptake by an irreversible chemical reaction (see Eqns. 17–19). Two families of curves are shown, the upper set corresponding to $D_H = 10^{-11}$ and the lower set corresponding to $D_H = 10^{-12}$ cm^2 s^{-1} (in both cases, the diffusion coefficients are constant). Note the damping effect on the diffusion profiles associated with increasing values of the kinetic rate constant k. The net effect of chemical reaction is to decrease the depth of steady-state H penetration.

irreversible chemical reaction. Failure to include a kinetic term in a diffusion model may result in estimates of diffusion coefficients that are too low. This principle can be easily seen in Fig. 9. As an example, the curve in Fig. 9 represented by $D_H = 10^{-12}$ cm^2 s^{-1} and $k = 0$ can alternatively be characterized by $D_H = 10^{-11}$ cm^2 s^{-1} and $k > 5 \times 10^{-4}$ s^{-1}. This example serves to illustrate that a correct estimate of a diffusion rate is dependent upon knowledge of the rate of irreversible uptake of a diffusing species, as for example, H uptake by framework hydrolysis reactions in feldspar altered layers.

3. DISCUSSION AND SUMMARY

Perhaps the most prominent and re-occurring point that can be drawn from the present study is that the steady-state diffusion of Na and H in leached/H-enriched layers in feldspars is relatively complex. This can be attributed to Na and H diffusion being coupled by ion exchange reactions, the presence of a moving boundary, the possibly nonconstant transport properties of the altered layers, and the effect of chemical reactions on H diffusion. Below some of the main conclusions regarding these factors are discussed.

One of the first requirements concerning the modeling of diffusion processes in leached/H-enriched layers is knowledge of whether the fluxes of elements diffusing both in and out of the near-surface altered structure have reached steady state. Low temperature dissolution experiments (i.e., at room temperature) often require several thousands of hours to reach steady-state conditions of dissolution, and by implication, steady-state diffusion of species within the leached/H-enriched layers. If steady-state conditions have not been attained, the diffusion model given by Eqn. 1 must be solved in its full form as a function of time, since $\partial C/\partial t \neq 0$. Nonsteady-state models have a particular utility in describing diffusion processes during the initial stages of dissolution, when the rates of diffusion $\gg$ rate of dissolution (i.e., diffusion rate $\gg$ rate of retreat of the fluid/solid interface).

Dissolution experiments run at elevated temperatures ($\geq$100°C) generally reach steady state in relatively short periods of time (see examples given in Part II). If steady state is achieved, then the simplifying assumption $\partial C/\partial t = 0$ can be applied to Eqn. 1. However, since leached/H-enriched layers do not attain an infinite thickness (as in Fig. 1, for example), Eqn. 1 must be modified to take into account that at steady state, the rate of advance of the leached/H-enriched zone into the bulk structure is counterbalanced by the rate of retreat of the fluid/solid interface. This condition is met by a diffusion model that includes a moving boundary term, as in Eqn. 4. In general terms, the inclusion of a separate moving boundary term in any steady-state diffusion model is important, since this ensures a mathematical coupling between two opposing processes, diffusion and dissolution.

Feldspars are a class of minerals where dissolution under most pH conditions leads to the preferential release of interstitial alkali and alkaline earth cations. At acid pH, the loss of interstitial cations is compensated for by the incorporation of H^+ (or H_3O^+) into the structure, thereby resulting in the formation of leached/H-enriched layers. The key question then becomes whether or not the inward and outward diffusion of species is coupled. If feldspar leached/H-enriched layers are modeled using constant, independent diffusion coefficients for H and Na, the resultant diffusion profiles display exponential behavior (see Figs. 2, 3). However, exponential curves do not allow for the presence of significant shoulders or plateaus representing extensive regions of either constant H enrichment or Na depletion (see Figs. 3, 4a; Part III).

Measured H and Na (or other alkali and alkaline earth cations) profiles in altered feldspars (see references cited earlier) generally display sigmoidal behavior, characterized by extensive plateau regions and steep diffusion fronts at depths close to the unaltered structure. This type of sigmoidal behavior is typically associated with an interdiffusion process. The ion exchange reaction between H^+ (or H_3O^+) from the solution and Na^+ in the structure results in a coupled diffusion process. If it is assumed that the inward and the outward diffusive fluxes are equal, then one single interdiffusion coefficient can be used for both species (e.g., Eqn. 7b). A diffusion model using an interdiffusion coefficient with a nonlinear concentration dependence, as in Eqn. 7b, results in sigmoidal diffusion profiles (see Figs. 5, 6). Sigmoidal profiles, in comparison to exponential profiles, are in much better accord with measured profiles for altered feldspars, as well as for many other altered silicates and glasses.

Even though some low temperature dissolution studies in the literature have diffusion profiles resembling exponential curves (due to a lack of significant shoulders or plateaus), these profiles generally have inflection points. This is evidence of sigmoidal behavior and nonconstant diffusion rates. The general conclusion that can be drawn from these observations is that whenever leached/H-enriched layers are formed in minerals by a process where the outward and inward fluxes of species are coupled, such as by an ion exchange process, then an interdiffusion coefficient should be used to model the diffusion of these species. The behavior of the resultant diffusion profiles will depend on the type of concentration dependence of the interdiffusion coefficient.

The H and Na profiles based on the simple interdiffusion model presented in this study are based on ratios of D_{Na}/D_H ranging from 10^{-2} to 10^5. It is important to note that D_{Na}/D_H ratios ≤ 1 yield exponential profiles, whereas sigmoidal profiles result when $D_{Na}/D_H > 1$. Even though the D_{Na}/D_H ratios were not measured in the present study, studies pertaining to glass alteration indicate that $D_{Na}/D_H \gg 1$ (see previously cited references). Given that the majority of feldspar alteration profiles in the literature are sigmoidal and that the synthetic alteration profiles presented in this study are sigmoidal when $D_{Na}/D_H > 1$, then it is reasonable to assume that outward alkali (alkaline earth) cation diffusion is faster than inward H diffusion. According to the modeling results, the most important criterion in determining depths of leaching/H-enrichment is the rate of diffusion of the slowest species, which is H. Changing the rate of diffusion of H by an order of magnitude changes the corresponding leaching/H enrichment depths by an order of magnitude, as well. For any given value of D_H, the overall depths of leaching/H enrichment also increase as a function of D_{Na}/D_H (see Figs.

5, 6), but the effect is not nearly as pronounced as changing solely the value of D_H.

Based on a qualitative comparison of the experimental data in Part III (see incomplete Na and H profiles in Figs. 3 and 4a, as well as RBS and ERDA data) with the synthetic H and Na profiles shown in Figs. 5 and 6a, an estimated lower limit for D_H can be determined, such that $D_H \geq 10^{-13}$ cm^2 s^{-1}. This estimate of D_H is based on depths of Na depletion and H enrichment that are on the order of 10,000–20,000 Å. In order for the alteration profiles to be sigmoidal, the ratio D_{Na}/D_H must be >1. If we add the additional constraint that the plateau depths of H enrichment and Na depletion extend to 10,000 Å (defined by the initial parts of profiles before the diffusion front, where $C_H \approx 1$ and $C_{Na} \approx 0$), this in turn necessitates ratios of $D_{Na}/D_H \geq 10^4$. The same constraint can be satisfied for $D_{Na}/D_H < 10^4$ if a structural factor is included in the interdiffusion model (see discussion below). At present, the assignment of more precise values for both D_H and the ratio D_{Na}/D_H is not defensible. This is mainly due to the incompleteness of the experimental curves presented in Part III, and the fact that any given synthetic diffusion profile requires two unknown fitting parameters, D_H and the ratio D_{Na}/D_H.

Despite the uncertainty in the diffusion rates of Na, these results are interesting in that they are in accord with extrapolated diffusion rates at 300°C of Na in albite glass (see Na diffusion curve for albite glass, reported in Fig. 11 of Part II; data from Jambon and Carron, 1976). This is potential evidence that the transport properties of the leached/H-enriched zone resemble those of an amorphous structure (i.e., albite glass).

One of the major unresolved questions is whether the transport properties of the leached/H-enriched layers are constant as a function of depth. This has an important bearing on diffusion rates for species diffusing through the leached/H-enriched zone. If it is assumed that the altered layers have a more open structure close to the fluid/solid interface, then it is reasonable to develop interdiffusion models with nonconstant diffusion coefficients. One approach to this is the use of a structural factor associated with an interdiffusion coefficient, as given by Eqn. 9. The use of such a structural factor imparts a significant degree of concentration dependence on the interdiffusion coefficient. As shown in Fig. 4, increasing the value of the structural factor increases the nonlinear behavior of the effective interdiffusion coefficient. Figures 7 and 8 reveal how, for a given set of values of D_H and D_{Na}/D_H, increasing the value of the structural factor (α) significantly increases the depth extents of the H enrichment and Na depletion. Thus, when comparing experimental results with a structural interdiffusion model, estimates for D_H and/or the ratio D_{Na}/D_H will be lower when $\alpha > 0$, as compared to the corresponding diffusion rates for $\alpha = 0$ (see diffusion rate estimates in previous discussion). Nonetheless, there is no precise experimental justification for assigning a precise value to α, such that at present it can only be used as a fitting parameter. At this point, it is not possible to resolve this problem.

An additional complication involving diffusional transport concerns the effects of condensation reactions. Condensation reactions involve the repolymerization of adjacent $\equiv$Si—OH groups as follows: $\equiv$Si—OH + HO—Si$\equiv$ → $\equiv$Si—O—Si$\equiv$ + H_2O. As was shown in Part III, there is indirect evidence for repolymerization within the leached/H-enriched region close to surface, at depths <700 Å for acid dissolution conditions. Repolymerization of the leached/H-enriched structure would serve to decrease rates of diffusion close to the surface. Thus, a more complete understanding and more accurate modeling of diffusional transport is dependent on knowledge of the effects due to potential repolymerization of the near-surface altered structure. Techniques, such as HRTEM, may be useful for determining structural changes within leached/H-enriched zones. Such information would be necessary for modeling changes in diffusional transport properties with depth.

From results in the present study, the lower limit for H diffusion can be constrained to $D_H \geq 10^{-13}$ cm^2 s^{-1} for dissolution conditions of 300°C and pH ~ 3.3–3.4 (note that the estimate for D_H may be lower if a structural factor is used). Based on the premise that $D_{Na}/D_H \gg 1$, Na diffusion coefficients should be significantly greater than 10^{-13} cm^2 s^{-1}. Estimates for D_{Na} in the present study are considerably more rapid than the Na diffusion rates reported in Part II, which are based on aqueous data at 300°C. In addition, extrapolation to 25°C, using the Arrhenius equation (based on E_a = 56 kJ/mol for Na diffusion in albite glass, from Jambon and Carron, 1976) results in $D_{Na} \gg 10^{-18}$ cm^2 s^{-1}; this is considerably faster than values reported in the literature at 25°C at similar acid pH conditions (see tabulated values in Chou and Wollast, 1984). One important point is that these comparisons suggest that aqueous data are of limited value for determining accurate diffusion coefficients in leached/H-enriched layers. Nonetheless, qualitative diffusion trends based on aqueous data may still be useful.

Chemical reactions may, or may not, have an effect on steady-state diffusion profiles. If the chemical reaction is reversible and faster than the rate of diffusion, then there is no net effect of the reaction on the steady-state diffusion profile of the reacting species. There will, however, be an effect on the evolution of the nonsteady-state diffusion profiles as a function of time. On the other hand, the effect of irreversible chemical reactions, such as associated with the uptake of H species during the hydrolysis of $\equiv$Al—O—Si$\equiv$ bonds, results in a damping effect on the associated steady-state H diffusion profiles (see Fig. 9). The importance of this result is that it shows that estimates of experimentally-determined diffusion rates may be too low if the effects of irreversible chemical reactions are not taken into account. It is difficult to estimate this effect in the present study, since the rates of hydrolysis within the altered zone at the experimental conditions given in Part III are not known. It is probable, however, that diffusion profiles will be more affected by irreversible chemical reactions during the initial, nonsteady-state period of dissolution, during which altered layers evolve the most rapidly.

A point related to the discussion above concerns itself with whether irreversible chemical reactions occurring within leached/H-enriched layers are responsible for the reported pH-dependence of diffusion rates, as has been suggested by Sjöberg et al. (1995). According to their results, H diffusion coefficients are pH invariant in the acid to neutral

pH range when diffusion rates are corrected for H uptake by chemical reaction. On the other hand, the pH dependency of diffusion rates may be real, as is postulated in this study. One reason for this is based on the assumption that transport rates of species are a function of the structural openness of the leached/H-enriched layers, which may be related to the pH conditions of dissolution. This argument is based on a more open structure being created at acid vs. neutral pH conditions, due to the greater degree of Na and Al preferential leaching, as well as a greater degree of H permeation (see discussion in Part III). Another possible factor that should be considered is related to whether the rates of diffusion are affected by the inherent charge of the leached layers. As discussed in detail in Part III, protonation and deprotonation reactions of ≡Si—OH and ≡Al—OH groups as a function of pH will determine the net charge of these groups, and this may have an influence on the rates of inward and outward diffusion of species within the altered zone. At present, these alternative explanations cannot be fully resolved until more is known about the detailed structure and chemistry of leached/H-enriched layers.

As mentioned previously, the incomplete nature of the experimentally-measured H and Na profiles in Part III is the main reason why no attempt was made to directly compare these profiles and fit them with theoretical curves. Nonetheless, it is important to compare real data with theory. Figure 10 shows such a comparison, between the acid pH Na RNRA profile (Fig. 4a, Part III) and several theoretical Na diffusion profiles based on a simple interdiffusion model ($D_H = 10^{-13}$ cm^2 s^{-1} and D_H/D_{Na} = 10, 10^2, and 10^3). Note that an analogous comparison with a measured H profile is not shown, simply due to the fact that the acid pH H profile only consists of a flat concentration plateau (see Fig. 3, Part III). As is quite evident in examining Fig. 10, there is a considerable mismatch between the measured profile and the theoretical curves shown. This mismatch is examined from two points of view.

The first point concerns itself with the RNRA measurements; their limitations are discussed in detail in Part III. Briefly, based on only one profile, there is no conclusive

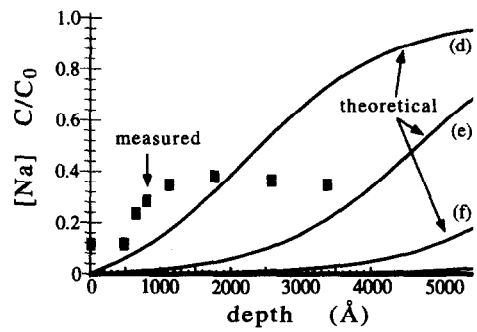

Fig. 10. Comparison of Na profile (acid pH) measured by RNRA (see Fig. 4a, Part III) with theoretical Na diffusion profiles. The theoretical profiles are based on the interdiffusion model given by Eqn. 8, with $D_H = 10^{-13}$ cm^2 s^{-1} and D_{Na}/D_H = 10, 10^2, and 10^3 (curves d, e, and f, respectively; these correspond to the same in Fig. 6a). See text for a discussion of the possible reasons for the different behavior of the measured diffusion profile.

proof that the sigmoidal behavior evidenced at shallow depths (<1000 Å) is real. It may be an artifact of the measurement or the sample. It should be recalled that the accurate determination of concentrations by RNRA depends on the stopping power of the material, and at shallow depths close to the surface, this may be poorly constrained, thereby leading to inaccuracies (Petit et al., 1990). This question can only be resolved with multiple measurements, and perhaps most importantly, with measurements utilizing another technique (such as SIMS). In addition to this, there is the general problem associated with the incompleteness of the Na and H profiles. Multiple measurements of profiles that encompass the complete extent of alteration are needed (depths > than 10,000 Å). Only when these conditions are fulfilled can one correctly compare and model deep H and Na alteration zones.

On the other hand, the experimental trend shown in Fig. 10 may also be real. The Na RNRA curves at acid and neutral pH (Fig. 4a, Part III) display weakly sigmoidal behavior before attaining concentration plateaus that are still well below that of the bulk material. This points to diffusion behavior that is potentially more complex than the modeled profiles presented here. The question then arises as to how the diffusion profiles evolve beyond these initial plateaus. One can speculate that it is possible that the Na concentration profiles (and possibly H, as well) may possess more than one plateau region, separated by sigmoidal changes in concentration. It is interesting to note that diffusion curves with this type of behavior have been noted in obsidian dissolution studies, where two H concentration plateaus were recorded (see Lee et al., 1974; Ericson et al., 1974). As noted by Ericson et al. (1974), multiple plateaus may signify the existence of more than one diffusion and binding mechanism for H species (i.e., water) during the dissolution process.

The idea of multiple diffusion mechanisms can be translated into multiple diffusion rates, such as would arise in leached/H-enriched layers composed of multiple layers, each with a distinct structure and corresponding transport property. Diffusion modeling of sandwich type composite materials yields profiles with multiple sigmoidal diffusion fronts (see extensive treatment of this in Crank, 1990). However, diffusion through a composite altered structure should not be considered to be the sole explanation for these types of a phenomena; other models may be just as valid. In any case, a better understanding of these problems points out the need for further research into the structure and transport properties of leached and H-enriched layers.

The theoretical diffusion profiles show that the altered layers leached in Na and enriched in H extend to depths of many thousands of Å. These chemically distinct altered layers are also deficient in Al, according to solution results (e.g., see Part II), as well as direct measurements (e.g., Hellmann et al., 1990). This implies that these altered layers have a radically different chemical composition as compared to unaltered albite. The results from Part III do not allow for a complete quantification of the stoichiometry of the altered layers created at acid pH conditions. However, a SIMS study of labradorite dissolution at acid pH conditions (Schweda and Sjöberg, 1997) yielded the following stoichiometry for altered layers created at pH 3.0: $H_{0.36}Si_{0.91}O_2$.

This stoichiometry results from the complete loss of Al and Ca from the altered zone. It is not unreasonable to suggest, by analogy, that the altered zone in albite (formed at pH 3.3) has a similar stoichiometry.

The question that can now be addressed is whether the presence of a thick altered zone with a stoichiometry similar to that given above can influence the overall rate of dissolution. The first point that must be considered is that the loss of Na and Al within the altered zone must change the crystallographic structure with respect to the bulk. It can be argued, despite the lack of experimental evidence, that the altered zone may have a more open structure, one that is permeable not only to H^+, but also perhaps to H_2O and H_3O^+ species. This potential openness is important in that it may increase the available number of hydrolysis sites on surface $\equiv$Si—OH groups that can be attacked, not from the front at the fluid/solid interface, but at bridging oxygen sites only accessible from within the altered zone. The net effect of this would be to increase the rate of detachment reactions of surface Si into solution. One can speculate even further by suggesting that detachment reactions are possible from perhaps much further into the altered layer, which implies that it may be possible to liberate not just individual $Si(OH)_4$ groups, but perhaps also larger entities, of the form $n \cdot Si(OH)_4$. This may be possible, if the altered layer structure is significantly weaker than the structure of albite, thereby making it susceptible to large-scale destruction via hydrolysis reactions. Evidence for the fragility of these altered layers is discussed by Schweda and Sjöberg (1997).

As one can note in the above discussion, the direct influence of leaching and H enrichment on the kinetics of dissolution is still speculative. Nonetheless, it also points out that much experimental, as well as theoretical work should be applied in this direction.

Acknowledgments—Many thanks are due to M. Dietrich for assistance and advice concerning the diffusion modeling using Maple® software. Discussions concerning diffusion in altered layers with L. Sjöberg were also useful. Lennart Sjöberg unexpectedly passed away in February, 1996. For those who knew him, we will miss his warmth and sense of humor. This paper is dedicated to the memory of the late Prof. David Crerar of Princeton University. This study benefited from the perceptive comments of S. Brantley, P. Brady, and an anonymous reviewer. This article is contribution no. 70 in the C.N.R.S.-DBT II program, Fluides dans la Croûte.

Editorial handling: J. D. Rimstidt

REFERENCES

Baucke F. G. K. (1974) Investigation of surface layers, formed on glass electrode membranes in aqueous solutions, by means of an ion sputtering method. *J. Non-Cryst. Solids* **14,** 13–31.

Berner R. A. and Holdren G. R., Jr. (1979) Mechanism of feldspar weathering-II. Observations of feldspars from soils. *Geochim. Cosmochim. Acta* **43,** 1173–1186.

Blum A. E. and Stillings L. L. (1995) Feldspar dissolution kinetics. In *Chemical Weathering Rates of Silicate Minerals* (eds. A. F. White and S. L. Brantley); *Reviews in Mineralogy,* Vol. 31, pp. 291–351. Mineralogical Society of America.

Boksay Z., Bouquet G., and Dobos S. (1967) Diffusion processes in the surface layer of glass. *Phys. Chem. Glasses* **8,** 140–144.

Boksay Z., Bouquet G., and Dobos S. (1968) The kinetics of the formation of leached layers on glass surfaces. *Phys. Chem. Glasses* **9,** 69–71.

Brady J. B. (1995) Diffusion data for silicate minerals, glasses, and liquids. In Mineral Physics & Crystallography *A Handbook of Physical Constants* (ed. T. J. Ahrens); *AGU Ref. Shelf* **2,** 269–290. AGU.

Brantley S. L. and Stillings L. (1996) Feldspar dissolution at 25°C and low pH. *Amer. J. Sci.* **296,** 101–127.

Busenberg E. and Clemency C. V. (1976) The dissolution kinetics of feldspars at 25°C and 1 atm CO_2 partial pressure. *Geochim. Cosmochim. Acta* **40,** 41–49.

Casey W. H., Westrich H. R., and Arnold G. W. (1988) Surface chemistry of labradorite feldspar reacted with aqueous solutions at pH = 2, 3, and 12. *Geochim. Cosmochim. Acta* **52,** 2795–2807.

Chou L. and Wollast R. (1984) Study of the weathering of albite at room temperature and pressure with a fluidized bed reactor. *Geochim. Cosmochim. Acta* **48,** 2205–2217.

Correns C. W. (1963) Experiments on the decomposition of silicates and discussion of chemical weathering. *Clays Clay Min.* **10,** 443–459.

Crank J. (1990) *The Mathematics of Diffusion.* Oxford Sci. Publ.

Darken L. S. (1948) Diffusion, mobility, and their interrelation through free energy in binary metallic systems. *Amer. Inst. Min. Metal. Engrs. Trans.* **175,** 184–201.

Doremus R. H. (1975) Interdiffusion of hydrogen and alkali ions in a glass surface. *J. Non-Cryst. Solids* **19,** 137–144.

Dran J.-C., Della Mea G., Paccagnella A., Petit J.-C., and Trotignon L. (1988) The aqueous dissolution of alkali silicate glasses: reappraisal of mechanisms by H and Na depth profiling with high energy ion beams. *Phys. Chem. Glasses* **29,** 249–255.

Ericson J. E., MacKenzie J. D., and Berger R. (1974) *Advances in Obsidian Glass Studies: Archaeological and Geochemical Perspectives* (ed. R. E. Taylor). Noyes Press.

Hartley G. S. and Crank J. (1949) Some fundamental definitions and concepts in diffusion processes. *Trans. Faraday Soc.* **45,** 801–818.

Hellmann R. (1994) The albite-water system: Part I. The kinetics of dissolution as a function of pH at 100, 200, and 300°C. *Geochim. Cosmochim. Acta* **58,** 595–611.

Hellmann R. (1995) The albite-water system: Part II. The time-evolution of the stoichiometry of dissolution as a function of pH at 100, 200 and 300°C. *Geochim. Cosmochim. Acta* **59,** 1669–1697.

Hellmann R., Eggleston C. M., Hochella M. F., Jr., and Crerar D. A. (1990) The formation of leached layers on albite surfaces during dissolution under hydrothermal conditions. *Geochim. Cosmochim. Acta* **54,** 1267–1281.

Hellmann R., Dran J.-C., and Della Mea G. (1997) The albite-water system: Part III. Characterization of leached and hydrogen-enriched layers formed at 300°C using MeV ion beam techniques. *Geochim. Cosmochim. Acta* **61,** 1575–1594.

Jambon A. and Carron J. P. (1976) Diffusion of Na, K, Rb, and Cs in glasses of albite and orthoclase composition. *Geochim. Cosmochim. Acta* **40,** 897–903.

Lanford W. A., Davis K., Lamarche P., Laursen T., and Groleau R. (1979) Hydration of soda-lime glass. *J. Non-Cryst. Solids* **33,** 249–266.

Lasaga A. C. (1979) Multicomponent exchange and diffusion in silicates. *Geochim. Cosmochim. Acta* **43,** 455–469.

Lee R. R., Leich D. A., Tombrello T. A., Ericson J. E., and Friedman I. (1974) Obsidian hydration profile measurements using a nuclear reaction technique. *Nature* **250,** 44–47.

Luce R. W., Bartlett R. W., and Parks G. A. (1972) Dissolution kinetics of magnesium silicates. *Geochim. Cosmochim. Acta* **36,** 35–50.

Muir I. J., Bancroft G. M., and Nesbitt H. W. (1989) Characteristics of altered labradorite surfaces by SIMS and XPS. *Geochim. Cosmochim. Acta* **53,** 1235–1241.

Muir I. J., Bancroft G. M., Shotyk W., and Nesbitt H. W. (1990) A SIMS and XPS study of dissolving plagioclase. *Geochim. Cosmochim. Acta* **54,** 2247–2256.

Pačes T. (1973) Steady-state kinetics and equilibrium between ground water and granitic rock. *Geochim. Cosmochim. Acta* **37,** 2641–2663.

Petit J.-C., Dran J.-C., Della Mea G., and Paccagnella A. (1989a)

Dissolution mechanisms of silicate minerals yielded by intercomparison with glasses and radiation damage studies. *Chem. Geol.* **78,** 219–227.

Petit J.-C., Dran J.-C., Paccagnella A., and Della Mea G. (1989b) Structural dependence of crystalline silicate hydration during aqueous dissolution. *Earth Planet. Sci. Lett.* **93,** 292–298.

Petit J.-C., Della Mea G., Dran J.-C., Magonthier M.-C., Mando P. A., and Paccagnella A. (1990) H-enriched layer formation during dissolution of complex silicate glasses and minerals. *Geochim. Cosmochim. Acta* **54,** 1941–1955.

Schweda P. and Sjöberg L. (1997) Near surface composition of acid-leached labradorite investigated by SIMS. *Geochim. Cosmochim. Acta* **61,** (in press).

Sjöberg L., Strandh H., and Schweda P. (1995) Diffusion of protons and cations in leached feldspar surface layers. *EUG 8 (Abstr.),* **7,** p. 65. Blackwell.

Smets B. M. J. and Lommen T. P. A. (1982) The leaching of sodium aluminosilicate glasses studied by secondary ion mass spectrometry. *Phys. Chem. Glasses* **23,** 83–87.

Wollast R. (1967) Kinetics of the alteration of K-feldspar in buffered solutions at low temperature. *Geochim. Cosmochim. Acta* **31,** 635–648.

Xiao Y. and Lasaga A. C. (1994) Ab initio quantum mechanical studies of the kinetics and mechanisms of silicate dissolution: H^+ (H_3O^+) catalysis. *Geochim. Cosmochim. Acta* **58,** 5379–5400.